Journal of Alloys and Compounds xxx (2014) xxx–xxx

Contents lists available at ScienceDirect

Journal of Alloys and Compounds

journal homepage: www.elsevier.com/locate/jalcom

Microstructure refinement and hardening of Ag–20 wt.%Cu alloy by rapid solidification

Danilo Lussana [a,*], Alberto Castellero [a], Maurizio Vedani [b], Dario Ripamonti [c], Giuliano Angella [c], Marcello Baricco [a]

[a] Dipartimento di Chimica and NIS, Università di Torino, Torino, Italy
[b] Dipartimento di Meccanica, Politecnico di Milano, Milano, Italy
[c] Istituto IENI-CNR, Unità territoriale di Milano, Milano, Italy

ARTICLE INFO

Article history:
Available online xxxx

Keywords:
Metals and alloys
Rapid-solidification
Mechanical properties
Microstructure
Phase transitions

ABSTRACT

Ag–20 wt.%Cu (wt%) hypoeutectic alloy has been rapidly solidified by means of planar flow casting technique. Two fcc solid solutions have been identified by X-ray diffraction. Microstructures have been observed by electron microscopy. A refinement of the eutectic microstructure, as well as of the Ag-rich primary phase, has been observed for high quenching rates, leading to a hardness value up to 235 Vickers. The lattice parameter and phase fraction of the Ag-rich solid solution increase as a function of quenching rates (i.e. wheel speed). The solidification processes occurring during rapid quenching have been described on the basis of thermodynamic and kinetic arguments.

1. Introduction

Silver–copper alloys are widely used for their electrical properties and, when the content of silver is higher than 80 wt%, for jewellery. In the latter case, the request for high hardness values is prevalent, since it improves wear resistance at the surfaces. The mechanical properties of these alloys are significantly influenced by the presence of eutectic microstructures, which arise from the solidification process [1]. In particular, a refinement of the microstructure with a consequent increase of hardness can be obtained by rapid solidification techniques such as copper mould casting, [1,2] and glass fluxing technique [3–5]. However, few data are available for these alloys prepared by means of melt spinning and planar flow casting techniques [6,7], which might lead to a microstructure refinement of eutectics down to the nanoscale, giving a further improvement of mechanical properties [8].

Aim of this study is to investigate the microstructure refinement and the consequent increase of hardness of a Ag–Cu jewellery alloy prepared by means of the planar flow casting technique. The solidification process can be described on the basis of the collected data and correlated to the significant improvement of hardness obtained.

2. Experimental

The starting material for this study consisted of a 3 mm thick plate of a Ag–20 wt.%Cu hypoeutectic alloy with commercial purity. Samples used as reference (zero-sample) were extracted from the plate, annealed for 5 h at 500 °C in order to eliminate structural defects induced during the production process, and then slowly cooled down to room temperature.

Ribbons were produced by means of planar flow casting (PFC) technique [9]. The as received material was induction melted in a boron-nitride crucible, under an inert helium atmosphere. Liquid alloy was then injected on a rotating copper wheel, with the surface located at 0.4 mm from the bottom of the crucible. Different cooling rates have been explored through casting ribbons with different wheel speeds: 10, 15, 20, 25 and 30 m s^{-1}. The average thickness ranged from 200 μm for the ribbon obtained at 10 m s^{-1}, to 100 μm for the ribbon prepared at 30 m s^{-1}. However, the thickness along each ribbon was not uniform, with relative variations around 30%. The higher the wheel speed, the larger the presence of macro defects such as holes and tears in the ribbons. In particular, for the ribbon prepared at 30 m s^{-1}, the surface defects were so severe that it could not be representative of the expected cooling rate, and thus it was excluded from the analysis.

The microstructure of the samples was investigated by means of optical and electron microscopy. Metallographic samples were prepared by grinding with emery papers, polishing down to 1 μm, and etching with a solution of 40% NH_3, 40% H_2O_2 and 20% ethanol. TEM samples, used also for some of the SEM analyses, were prepared by ion milling. SEM investigations were performed with a Hitachi SU-70 TFEG microscope equipped with EDS. Backscattered (BEI) and secondary electron imagining (SEI) micrographs were taken with an acceleration voltage of 15 kV, the same condition used for EDS analyses. TEM observations were carried out with a Philips CM-200 TFEG, operating at 200 kV.

X-ray diffraction (XRD) analyses were carried out with a Panalitycal X'pert diffractometer, with Cu Kα radiation. Structural and microstructural information has been obtained by means of Rietveld analysis [10] using the Maud software [11].

Mechanical properties were evaluated by instrumented indentation. The Vickers hardness was measured imposing a maximum penetration depth of 2 μm with a load controlled Fisherscope HM2000.

* Corresponding author. Tel.: +39 011 670 7569.
E-mail address: danilo.lussana@unito.it (D. Lussana).

0925-8388/$ - see front matter © 2014 Elsevier B.V. All rights reserved.
http://dx.doi.org/10.1016/j.jallcom.2014.01.054

3. Results

Fig. 1 shows the grain structure of cross sections of a ribbon quenched with a wheel speed of 10 m s^{-1}. An evident feature, common to all ribbons, is the presence of two solidification fronts, one starting from the wheel side and the other from the air side, which meet in the central region of the ribbon (Fig. 1a). In some cases, especially when the ribbon thickness is large, a zone with a microstructure characterized by large grains forms between the two solidification front (Fig. 1b). The presence of two solidification fronts suggest similar heat extraction rates from the wheel surface and the air one, while a higher rate was expected on the wheel side. The partial immiscibility of silver and copper might lead to a low wettability of the liquid on the copper wheel. This effect, in turn, is supposed to created a non-uniform flow of the melt and then it likely reduced the heat extraction rate.

As expected, the grains have grown in a direction perpendicular to the wheel side. The microstructure appears rather fine, so that it is difficult to clearly identify columnar grains.

In order to have a global view of the structure of each ribbon, X-ray diffraction analyses were performed. Fig. 2 shows the diffraction patterns obtained from the wheel side and from the air side of the ribbons. Only the reflections of the silver-rich fcc phase (α) and the copper rich fcc phase (γ) are present. A simple comparison between the expected intensities of the α phase and those observed experimentally reveals the presence of preferential grain growth, mainly along the ⟨100⟩ direction (in agreement with the preferential solidification direction in fcc alloys). The ribbons shows broader peaks in comparison to those of the zero-sample, suggesting the formation of a defective structure with reduced grain sizes due to rapid solidification. Moreover, the diffraction peaks of the α phase of the ribbons are shifted towards higher angles, indicating a decrease of the lattice constant when increasing the wheel speed (Fig. 3a).

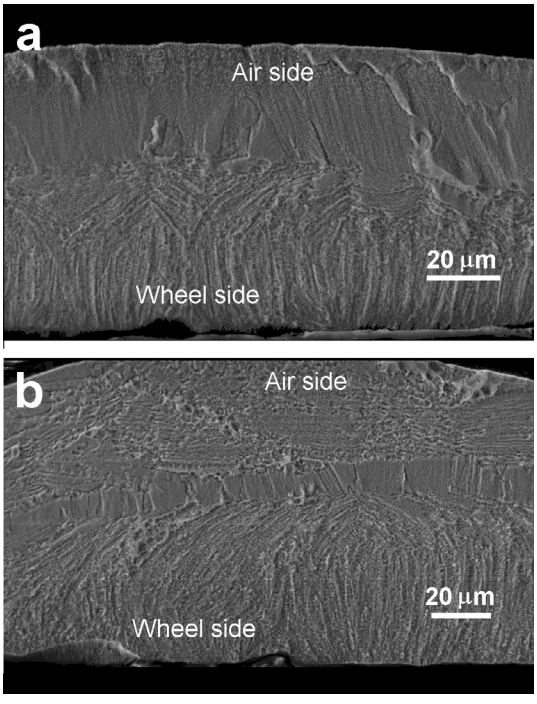

Fig. 1. SEM images of the cross section of Ag–20 wt.%Cu ribbon quenched at 10 m s^{-1} showing the two solidification fronts meeting at the middle of the sample (a) and forming a central zone with large grains (b).

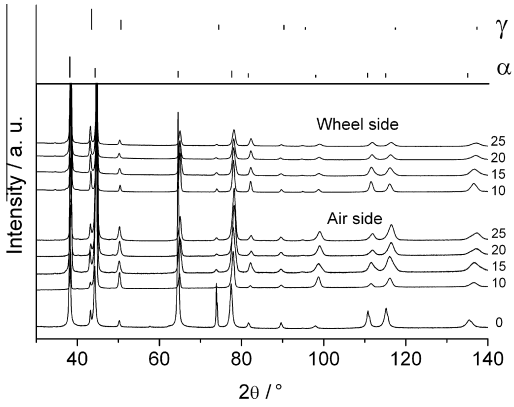

Fig. 2. XRD patterns of Ag–20 wt.%Cu zero-sample and of the air and wheel side of the ribbons quenched at the indicated wheel speeds. Peak position and relative intensity of α and γ phases are shown for comparison.

Conversely, the lattice parameter of the γ phase remains almost unchanged as a function of the quenching rate (Fig. 3a). The small fraction of the γ phase in the sample makes the lattice constant evaluation affected by a larger uncertainty in comparison to that of the α phase. For all the conditions examined, the differences of the lattice parameters calculated from the wheel side and from the air side of the same ribbon are rather small, suggesting a similar process for the two solidification fronts.

The quantities of solute dissolved in fcc solid solutions (that is, copper in α and silver in γ phases) have been evaluated comparing the refined lattice parameters with data from Ref. [12]: the latter were fitted according to a parabolic law, obtaining a relation between lattice parameter and alloy composition. The value of copper retained in the silver-rich α phase (Fig. 3b) is nil for the zero-sample, corresponding to the expected value for a sample close to the thermodynamic equilibrium. On the contrary, the rapid quenching significantly increases the quantity of copper in the α phase, which progressively grows from about 3.5 wt% for the ribbon quenched at 10 m s^{-1} up to about 5.0 wt% of the ribbon prepared at 25 m s^{-1}. The values of the lattice parameter for the γ phase indicate that the Ag content in the copper-rich γ phase is roughly constant (about 3.0 wt%).

The difficulty of modelling the preferential orientations rising from the complex microstructure hinders the calculation of phase quantities directly through Rietveld analysis. For this reason, an indirect approach has been used. Starting from the values reported in Fig. 3b and being constant the alloy composition, it was possible to calculate, performing a mass balance, the total amount of the α phase in the ribbons as a function of the wheel speed (Fig. 3c). The value of zero-sample is again close to the expected thermodynamic equilibrium value (80 wt%). The fraction of α phase increases progressively with the increase of the solidification rate.

The microstructures observed in the various samples are rather inhomogeneous, even inside the same sample. However, two main microstructures can be identified. One is typical of low wheel speeds (10 and 15 m s^{-1}) and a second one is characteristic of high wheel speeds (20 and 25 m s^{-1}). Fig. 4a shows the typical feature of a ribbon prepared at low quenching rate (i.e. 10 m s^{-1}), characterized by the presence of α primary phase, together with an eutectic microstructure. The eutectics consist of silver- and copper-rich lamellae that, in some zones, are almost regular whereas, in some other areas, are rather irregular, with diverging directions of growth. The lamellae thickness is not homogeneous, ranging about about from 200 μm down to 20 nm. The EDS analysis of the α primary phase shows a quantity of Cu close to 3 wt%. However, at high magnification (Fig. 4b), Cu-rich nanosized particles are

Please cite this article in press as: D. Lussana et al., J. Alloys Comp. (2014), http://dx.doi.org/10.1016/j.jallcom.2014.01.054

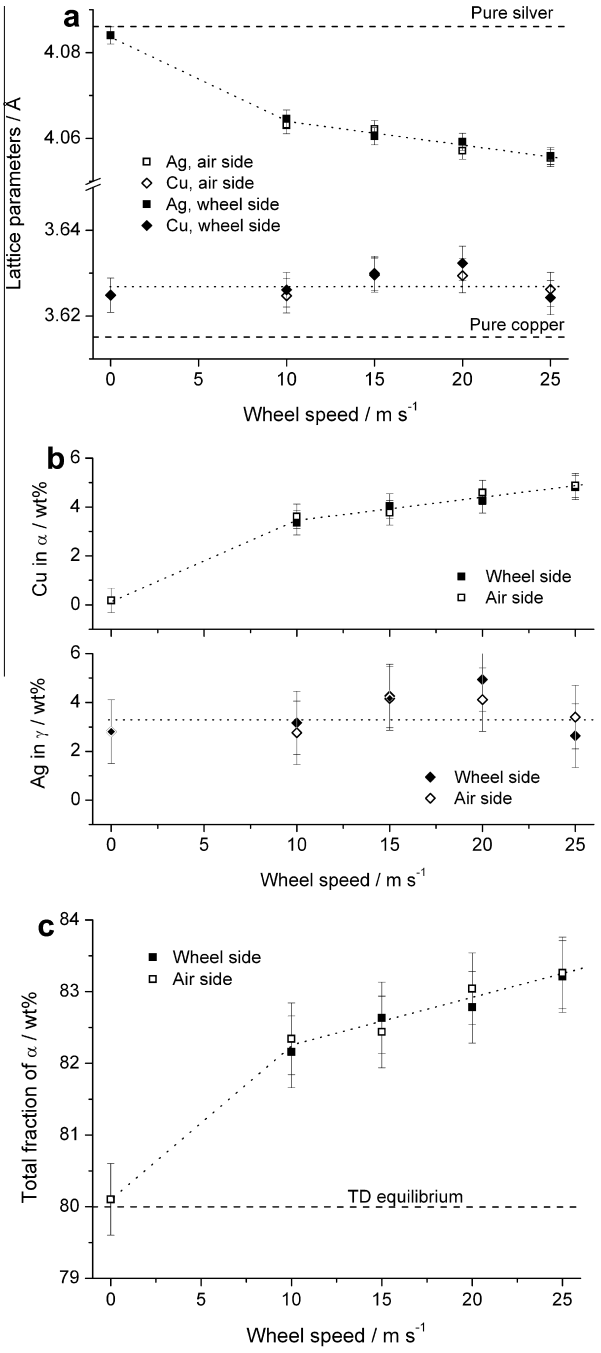

Fig. 3. Lattice parameter (a), solute content (b) and α phase fraction (c) as a function of the wheel speed for Ag–20 wt.%Cu rapidly quenched ribbons.

visible inside the α phase. Fig. 4c shows the typical microstructure of a ribbon from high quenching rates (i.e. 20 m s^{-1}). Fine eutectics and the α primary phase are present, but the latter shows a fine dendritic microstructure. In Fig. 4d bright field (BF) TEM micrograph of a typical eutectic region of a ribbon at 10 m s^{-1} is reported with zone axis ***B*** close to [0 1 1]. The TEM observation through $\boldsymbol{B} \approx [0\,1\,1]$ allows on-edge observation of the α and γ phase lamellae in the eutectic product and, therefore, an estimation of the lamellae thickness. TEM analyses (not reported here) also show that all ribbons present a significantly higher dislocation density in comparison to the zero-sample.

The hardness of the Ag–20 wt.%Cu alloy shows a significant increase from the zero-sample (about 85 Vickers) to the rapid solidified samples, as shown in Fig. 5. The hardness of the ribbons increases progressively from about 150 Vickers for the ribbon prepared at 10 m s^{-1} up to 235 Vickers for the ribbon quenched at 25 m s^{-1}, and it is significantly higher than the maximum value reported for the commercial "800 Silver" jewellery alloy (about 100 HV) [13]. Moreover, the ribbons maintain an interesting level of ductility (fracture strain around 3%) as shown by tensile tests (not reported here).

4. Discussion

In order to analyze the data collected on the Ag–20 wt.%Cu alloy prepared by PFC technique, the first aspect to take into account is the inhomogeneous quenching rate explored by each sample. This fact is related to an imperfect flow of the melt on the surface of the wheel, and it is clearly evident from the thickness variations inside the same ribbon. An estimation of the different undercooling values reached during solidification can be obtained from the average thickness of the eutectic lamellae. It is expected that it decreases with increasing solidification rate. However, on the same sample, and in particular on the ribbon at 10 and 15 m s^{-1}, the interlamellar spacing ranges from about 100 to 20 nm. Considering that it is proportional to $(\Delta T_0)^{-1}$ [13], where ΔT_0 is the undercooling, it can be concluded that different zones of the same sample experienced undercooling that likely differs by a factor of 3. On the other hand, XRD results, as well as the hardness measurements, are representative of an average behaviour of investigated samples.

The microstructure reported in Fig. 4a is representative of ribbons prepared at 10 and 15 m s^{-1}, but some zones with a microstructure similar to that of Fig. 4c are also present in the same samples. On the contrary, the ribbons quenched at 20 and 25 m s^{-1} present only the morphology reported in Fig. 4c. The observed eutectic microstructures can be explained according to the classical solidification mechanism for eutectics proposed by Kurz and Fisher [13]. The high quantity of solute at the eutectic composition for the Ag–Cu system (that is: 29.5 wt% of Cu) favours the formation of a lamellar microstructure instead of a fibrous one, as evidenced by the SEM images (Fig. 4). Moreover, the low entropy of fusion of silver and copper, equal to 9.2 and 9.8 J mol^{-1} K^{-1}, respectively, favours the formation of regular eutectics. However, SEM images show the presence of both regular and irregular eutectics, the latter with a diverging direction of growth of lamellae, together with some branching. This fact can be explained by the high solidification rate which did not allow a diffusion of solute fast enough to let the lamellae grow in a regular arrangement.

Under equilibrium condition, the total fraction of α phase in the alloy should be 80 wt%, as actually observed for the zero-sample (Fig. 3c). The measured quantities of α phase in rapidly quenched ribbons are higher, ranging from 82% (10 m s^{-1}) to 85% (25 m s^{-1}).

The experimental results related to the as quenched ribbons reveal that the solute content in α and γ phases and the α phase fraction are lower than those expected at the eutectic temperature and higher than those expected at room temperature.

The presence of nanoparticles of γ phase inside the dendrites of the primary α phase (Fig. 4b) can be interpreted in terms of solid state precipitation, according to the solvus curve of the binary phase diagram [14]. Due to the high cooling rate and to the slowing down of diffusivity upon cooling, the thermodynamic equilibrium could not be attained during the whole cooling process.

In the case of α phase, the increased Cu content with the wheel speed (i.e. cooling rate) indicates a higher supersaturation of the solid solution induced by the higher level of undercooling, that also leads to the retention of a larger amount of the α phase with respect to the equilibrium.

In the case of γ phase, the Ag content appears to be independent on the wheel speed (i.e. cooling rate). This behavior can be related,

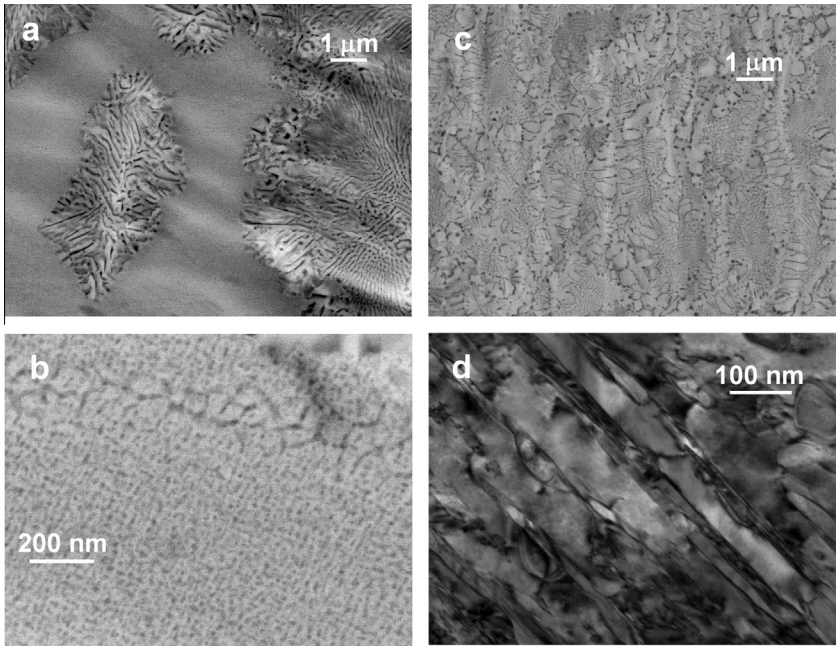

Fig. 4. SEM images of a Ag–20 wt.%Cu ribbon quenched at 10 m s^{-1} showing a primary phase and eutectics (a). An enlargement of the a primary phase shows fine Cu-rich particles (b). SEM image of a Ag–20 wt.%Cu ribbon quenched at 20 m s^{-1} showing a dendritic primary α phase and eutectics (c). TEM image of typical eutectic microstructure (d).

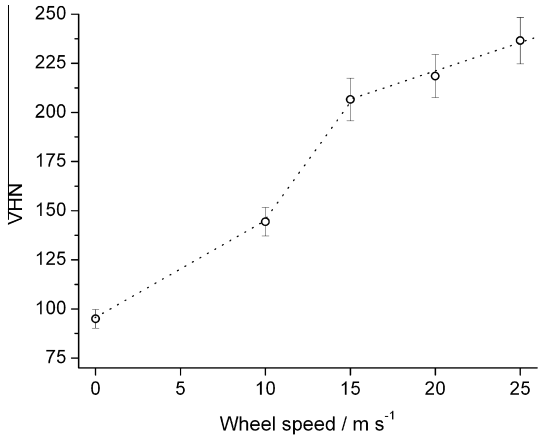

Fig. 5. Vickers hardness of rapidly solidified Ag–20 wt.%Cu alloy as a function of the wheel speed. Dotted line is a guide for the eyes.

on the one hand, to the lower accuracy of the Rietveld refinement due to the small amount of γ, and, on the other hand, to diffusion effects. In fact, the interdiffusion coefficient for Cu–2 wt.% Ag [15] is smaller than that for Ag–2 wt.% Cu [16]. This means that atomic mobility in γ phase is more difficult than in α phase. In addition, diffusion in γ phase slows down at higher temperature with respect to that of α phase. Thus, considering the same degree of undercooling for the two phases, the effect of the cooling rate on the solute content in γ phase is less relevant and the Ag content remains almost constant, independently on the wheel rate.

The refinement of the microstructure obtained by PFC leads to significant increase of hardness of the ribbons, when compared to the zero-sample. Two contributions are responsible for this result: on one hand, a high dislocation density has been introduced and, on the other hand, the eutectic microstructure has been significantly refined. It is worth noting that the lamellar spacing reported in the literature for similar alloys prepared by rapid solidification reached a minimum value of about 50 nm [1,17,18] whereas, in the ribbons prepared at 20 and 25 m s^{-1}, it reached values below 20 nm. A further increase of hardness can be attributed to the refinement of the microstructure of the α primary phase, which forms sub-micrometric dendrites for high undercoolings. For comparison, as quenched Ag–Cu solid solutions with 6–7.5 wt.% Cu show hardness between 43 HV and 47 HV [13,19], indicating that the contribution to the measured hardness from the primary solid solution is limited. Additionally, pure silver [20] cast by PFC showed a moderate increase of hardness (from about 45 to 65 Vickers) with respect to the alloy studied here (from 85 to 235 Vickers). In the former case, a contribution to the strengthening comes only from the grain size refinement of the α phase and from the introduction of structural defects. Indeed, the increase of hardness observed in pure silver is comparable to that observed in Ag–20 wt.%Cu ribbons from 15 to 25 m s^{-1}. In the case of the alloy, the eutectic microstructures justify not only the higher hardness value of the zero-sample, but also the larger relative increase due to the significant refinement of the lamellar spacing.

5. Conclusions

Ribbons of Ag–20 wt.%Cu alloy prepared by means of planar flow casting technique show a significant increase of hardness, changing from 80 Vickers of an annealed sample to about 230 Vickers for ribbons. This improvement is due to the introduction of dislocations and to the refinement of the microstructure. In particular, the eutectic microstructures show interlamellar spacing values down to 20 nm. For the ribbons prepared with high quenching rates (i.e. high wheel speed), the Ag-rich primary α phase shows a dendritic microstructure with sub-micrometric dimensions which allow a further increase of hardness.

Acknowledgments

This work has been financially supported by MIUR (PRIN 2008YNZB7 M-002). Dr. Brunella, Department CMIC, Politecnico

di Milano, is truthfully acknowledged for her support on TEM observations.

References

[1] Y.Z. Tian, Z.F. Zhang, Scripta Mater. 66 (2012) 65–68.
[2] E.M. Park, G.A. Song, J.K. Lee, M.H. Lee, H.S. Lee, J.Y. Park, N.S. Lee, Y. Seo, K.B. Kim, J. Alloys Comp. 509 (2011) 9015–9018.
[3] S. Walder, P.L. Ryder, J. Appl. Phys. 74 (1993) 6100–6106.
[4] S. Zhao, J.F. Li, L. Liu, Y.H. Zhou, Mater. Charact. 60 (2009) 519–524.
[5] S. Zhao, J.F. Li, L. Liu, Y.H. Zhou, J. Cryst. Growth 311 (2009) 1387–1391.
[6] J. Dutkiewicz, L. Lityfiska, R. Swiatek, Int. J. Mater. Prod. Technol. 53 (1995) 131–138.
[7] D.J. Thoma, T.K. Glasgow, S.N. Tewari, J.H. Perepezko, N. Jayaraman, Mat. Sci. Eng. 98 (1988) 89–93.
[8] M. Baricco, E. Bosco, E. Olivetti, M. Palumbo, P. Rizzi, A. Stantero, L. Battezzati, Int. J. Mater. Prod. Technol. 20 (2004) 358–376.
[9] P.D. Wilde, E.F. Matthys, Mat. Sci. Eng. A 150 (1992) 237.
[10] R.A. Young, The Rietveld Method, Oxford University Press, New York, 1993.
[11] L. Lutterotti, S. Matthies ,H. -R. Wenk, in: Proceeding of the Twelfth International Conference on Textures of Materials (ICOTOM-12), vol. 1, 1999, pp. 1599.
[12] W.B. Pearson, A Handbook Of Lattice Spacings And Structures Of Metals And Alloys – 2, Pergamon Press, Oxford, 1967, p. 514.
[13] ASM Handbook, Properties and Selection: Nonferrous Alloys and Special-Purpose Materials (electronic version), ASM International, Materials Park (OH), vol 2, 1997, pp. 2038
[14] F.H. Hayes, H.L. Lukas, G. Effenberg, G. Petzow, Z. Metallkde 77 (1986) 749–754.
[15] H. Oikawa, H. Takei, S. Karashima, Metall. Trans. 4 (1973) 653–655.
[16] G. Barreau et al., Mem. Sci. Rev. Met. 68 (1971) 357–366.
[17] Y.Z. Tian, J.J. Li, P. Zhang, S.D. Wu, Z.F. Zhang, M. Kawasaki, T.G. Langdon, Acta Mater. 60 (2012) 269–281.
[18] J.B. Liu, Y.W. Zeng, L. Meng, J. Alloys Comp. 464 (2008) 168–173.
[19] S. Colombo, P. Battaini, G. Airoldi, J. Alloys Comp. 437 (2007) 107–112.
[20] D. Lussana, A. Castellero, D. Ripamonti, G. Angella, M. Vedani, A. Zambon, M. Baricco, Int. J. Mater. Res. 103 (2012) 1117.